Journal of Ethnopharmacology 239 (2019) 111918

Contents lists available at ScienceDirect

Journal of Ethnopharmacology

journal homepage: www.elsevier.com/locate/jethpharm

Calligonum comosum (Escanbil) extract exerts anti-angiogenic, anti-proliferative and anti-inflammatory effects on endometriotic lesions

Kiandokht Kiani[a,b,c], Jeannette Rudzitis-Auth[c], Claudia Scheuer[c], Mansoureh Movahedin[d,**], Seyede Nargess Sadati Lamardi[e], Hossein Malekafzali Ardakani[f], Vivien Becker[c], Ashraf Moini[b,g], Reza Aflatoonian[b], Seyed Nasser Ostad[h], Michael D. Menger[c], Matthias W. Laschke[c,*]

[a] Vali-e-Asr Reproductive Health Research Center, Tehran University of Medical Sciences, Tehran, Iran
[b] Department of Endocrinology and Female Infertility, Reproductive Biomedicine Research Center, Royan Institute for Reproductive Biomedicine, ACECR, Tehran, Iran
[c] Institute for Clinical & Experimental Surgery, Saarland University, 66421, Homburg/Saar, Germany
[d] Anatomical Sciences Department, Faculty of Medical Sciences, Tarbiat Modares University, Tehran, Iran
[e] Department of Traditional Pharmacy, School of Persian Medicine, Tehran University of Medical Sciences, Tehran, Iran
[f] Epidemiology and Biostatistics Department, School of Public Health, Tehran University of Medical Sciences, Tehran, Iran
[g] Department of Gynecology and Obstetrics, Arash Women's Hospital, Tehran University of Medical Sciences, Tehran, Iran
[h] Department of Toxicology & Pharmacology, Faculty of Pharmacy, Tehran University of Medical Sciences, Tehran, Iran

ARTICLE INFO

Keywords:
Endometriosis
Calligonum comosum
Angiogenesis
Vascularization
Inflammation
Proliferation

ABSTRACT

Ethnopharmacological relevance: *Calligonum comosum* is a desert plant that is applied in traditional folkloric medicine for the treatment of abnormally heavy or prolonged menstruation and menstrual cramps. Moreover, it has been suggested for the treatment of infertility-causing conditions. Its bioactive chemical constituents inhibit multiple processes, such as angiogenesis, inflammation and invasive tissue growth, which may be beneficial in the therapy of endometriosis.

Aim of the study: We investigated the effects of *Calligonum comosum* on the development of endometriotic lesions.

Materials and methods: We evaluated the anti-angiogenic activity of *Calligonum comosum* ethyl acetate fraction (CCEAF) in different *in vitro* angiogenesis assays. Moreover, we surgically induced endometriotic lesions in BALB/c mice, which received 50 mg/kg *Calligonum comosum* total extract (CCTE) or vehicle (control) over 4 weeks. The growth, cyst formation, vascularization and immune cell infiltration of the lesions were assessed with high-resolution ultrasound imaging, caliper measurements, histology and immunohistochemistry.

Results: CCEAF doses of up to 10 µg/mL did not impair the viability of human dermal microvascular endothelial cells (HDMEC), but dose-dependently suppressed their migration, tube formation and sprouting, indicating a substantial anti-angiogenic effect of CCEAF. Furthermore, CCTE significantly inhibited the growth and cyst formation of developing murine endometriotic lesions when compared to vehicle-treated controls. This was associated with a reduced vascularization, cell proliferation and immune cell infiltration.

Conclusions: Our findings show that *Calligonum comosum* targets multiple, fundamental processes in the pathogenesis of endometriosis, which may be beneficial for the treatment of this common gynecological disorder.

1. Introduction

Endometriosis is one of the most common benign disorders, which affects 6–10% of women in reproductive age (Giudice and Kao, 2004). The disease is characterized by the presence of ectopic endometrial tissue with glands and stroma outside the uterine cavity. Endometriosis patients often suffer from dysmenorrhea, dyspareunia, dysuria and chronic abdominal or pelvic pain as well as infertility, resulting in a markedly limited quality of life (Adamson, 2011).

Current therapeutic options for endometriosis are not satisfactory. In fact, pharmacological long-term treatment with anti-estrogenic agents bears the risk of severe side effects, such as depression or osteoporosis (Crosignani et al., 2006). Moreover, surgical removal of endometriotic lesions is associated with high recurrence rates (Cheong

* Corresponding author.
** Corresponding author.
E-mail addresses: movahed.m@modares.ac.ir (M. Movahedin), matthias.laschke@uks.eu (M.W. Laschke).

https://doi.org/10.1016/j.jep.2019.111918
Received 3 November 2018; Received in revised form 10 April 2019; Accepted 23 April 2019
Available online 26 April 2019
0378-8741/

et al., 2008). Hence, there is an urgent need for the identification of novel compounds that promote the regression of endometriotic lesions without inducing severe side effects. A continuously increasing number of studies suggest that such compounds may be found in the field of traditional herbal medicine (Wieser et al., 2007; Rudzitis-Auth et al., 2012, 2013; Ricci et al., 2013).

Although the etiology of endometriosis still remains a matter of debate (Burney and Giudice, 2012), there is general consensus that multiple biological processes, such as angiogenesis and vasculogenesis (Laschke and Menger, 2012; Laschke and Menger, 2018), inflammation (Jiang et al., 2016), oxidative stress (Scutiero et al., 2017) and invasive tissue growth (Jiang and Wu, 2012) contribute to its complex pathophysiology. Accordingly, pleiotropic compounds simultaneously targeting these processes may be particularly suitable for the prevention and eradication of endometriotic lesions.

Calligonum is a plant genus in the family *Polygonaceae* with about 80 species across the Mediterranean region, Asia and North America. *Calligonum comosum,* also known as *Escanbil*, can be found in the desert areas of Khozestan, Sistan and Baluchestan, Semnan, Kerman and Yazd provinces of Iran (Ranjbarfordoei et al., 2013). In traditional folkloric medicine, *Calligonum comosum* is applied for the treatment of abnormally heavy or prolonged menstruation and menstrual cramps. Moreover, it has been suggested for the treatment of infertility-causing gynecological disorders, such as polycystic ovary syndrome (Tahmasebi et al., 2018). *Calligonum comosum* exhibits a broad effect spectrum with anti-oxidant, anti-inflammatory and anti-cancer activity (El-Hawary and Kholief, 1990; Liu et al., 2001; Badria et al., 2007; Alwakeel, 2008; Hammami et al., 2011; Ali et al., 2012; Abdallah et al., 2014). These effects are mediated by different bioactive chemical constituents, including tannins and several anti-oxidative flavonoids, such as quercetin and kaempferol, as well as their glycoside derivatives astragalin, taxifolin, (+)-catechin and dehydrodicatechin A (EI Sayyad and Wagner, 1978; Samejo et al., 2011; Ahmed et al., 2016; Cheruth et al., 2016).

Based on these findings, we investigated how this broad effect spectrum of *Calligonum comosum* affects the development of endometriotic lesions. We first evaluated the anti-angiogenic action of *Calligonum comosum* in different *in vitro* angiogenesis assays. In addition, we surgically induced endometriotic lesions in *Calligonum comosum*- and vehicle-treated BALB/c mice and assessed their growth, cyst formation, vascularization and immune cell infiltration using high-resolution ultrasound imaging, caliper measurements, histology and immunohistochemistry over an observation period of 4 weeks.

2. Materials and methods

2.1. Plant material and extract preparation

Aerial parts of *Calligonum comosum (Escanbil),* including new stems, leafs, flowers and fruits were collected in the local area of Esfahan province, Iran, at blossom time (May to June 2014). A voucher specimen was stored at Kashan Botanical Garden Herbarium, Iran, with the accession number KBGH 1101.

The collected parts were separately dried in the shade at room temperature for 4 weeks. Based on previous activity testing of different types of *Calligonum comosum* extract (Kiani et al., 2016), 1 kg of the plant (500 g: mixture of new stems, leafs and flowers; 500 g: fruits) was powdered with a grinder and soaked in 70% aqueous ethanol (Merck, Darmstadt, Germany) three times in a time interval of 3 days at room temperature. The excessive solvent was evaporated with a rotary vacuum evaporator (60 rpm at 40 °C) and a vacuum oven to obtain a condensate total extract (150 g). We used this final *Calligonum comosum* total extract (CCTE) for the *in vivo* experiments. In addition, 100 g of CCTE were further fractionated with hexane, chloroform and ethyl acetate. This *Calligonum comosum* ethyl acetate fraction (CCEAF) was used for the *in vitro* assays.

2.2. Cell culture

For our *in vitro* angiogenesis assays, we used human dermal microvascular endothelial cells (HDMEC; PromoCell, Heidelberg, Germany). The cells were cultured in ECGM-MV medium (PromoCell) at 37 °C in a humidified atmosphere and 5% CO_2. A stock solution of CCEAF (100 mg/mL dissolved in dimethyl sulfoxide (DMSO; Sigma-Aldrich, Taufkirchen, Germany) was stored at −20 °C. For the experiments, the stock solution was further diluted with the cell culture medium, resulting in CCEAF concentrations of 0.01–100 µg/mL. CCEAF- and vehicle-treated cells were exposed to identical DMSO end volumes.

2.3. Viability assays

A water-soluble tetrazolium (WST)-1 assay (Roche diagnostics, Mannheim, Germany) and a lactate dehydrogenase (LDH) assay (Cytotoxicity Detection Kit PLUS; Roche diagnostics) were performed to study the effect of CCEAF on the viability of HDMEC. For this purpose, 3×10^4 HDMEC in 100 µL of culture medium per well were seeded in 96-well plates and exposed to vehicle (DMSO; Sigma-Aldrich; control), 1% Triton X-100 (Carl Roth GmbH, Karlsruhe, Germany) as cytotoxic control or different concentrations of CCEAF (0.01, 0.1, 1, 10, 50, 100 µg/mL). After 24 h, 10 µL of WST-1 reagent (60 min incubation at 37 °C) or 100 µL LDH reaction solution (10 min incubation at room temperature in the dark followed by 50 µL stop solution) per 100 µL medium were pipetted to each well. Subsequently, we measured the absorption at 450 nm (WST-1 assay) or 492 nm (LDH assay) with 620 nm as reference by means of a microplate reader (PhoMo; Anthos Mikrosystem GmbH, Krefeld, Germany) and corrected it to blank values. The experiments were performed in quadruplicate.

2.4. Cell migration assays

A transwell migration assay and a scratch wound healing assay were used to analyze the effect of CCEAF on the migration of HDMEC. The transwell migration assay was performed in a 24-well chemotaxis chamber containing inserts with polycarbonate membranes with 8 µm-pores (Corning Costar by VWR, Darmstadt, Germany). HDMEC were exposed to 1 or 10 µg/mL CCEAF or vehicle (DMSO; control) for 24 h. Thereafter, 1×10^5 of the treated cells in 250 µL fetal calf serum (FCS)-free ECGM-MV (PromoCell) were transferred into a 24-well insert and 750 µL ECGM-MV with 1% FCS (Biochrom, Berlin, Germany) was pipetted to the lower well. The chamber was incubated at 37 °C in a humidified atmosphere with 5% CO_2 for 6 h. Then, the cells on the top of the transwell membrane were removed completely with a cotton swab and the migrated cells on the bottom of the transwell membrane were fixed with methanol and stained with Dade Diff-Quick (Dade Diagnostika GmbH, München, Germany). The number of migrated cells was counted in 20 microscopic regions of interests (ROIs) at 20× magnification (BZ-8000; Keyence, Osaka, Japan) and is given as cells/ROI. The experiments were performed in quadruplicate.

For the scratch wound healing assay, 2×10^5 HDMEC per well were transferred on a 24-well plate and left overnight to attach and reach confluency. The cell layer was then scratched by means of a 10 µL pipet tip. Cell debris was washed away from the scratch wounds with phosphate-buffered saline (PBS). The cells were then exposed to 1 and 10 µg/mL CCEAF or vehicle (DMSO; control). Images were recorded directly after scratching (0 h) as well as after 6, 12 and 24 h with a Leica DMIL microscope and a digital microscope camera (Leica DFC450 C; Leica Microsystems, Wetzlar, Germany). Wound areas (in % of the original wound area) were measured using the LAS V4.8 software (Leica DFC450 C; Leica Microsystems, Wetzlar, Germany). A total number of 12–14 wound areas per experimental group were analyzed.

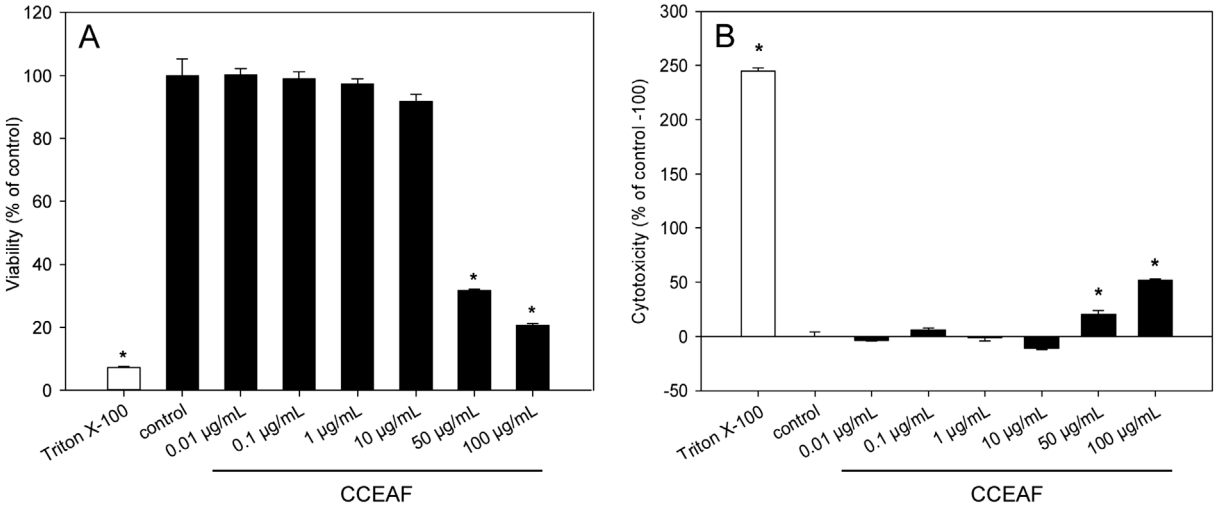

Fig. 1. In vitro toxicity of CCEAF. A, B: Viability (% of control) of HDMEC (A) and cytotoxicity (% of control-100) of CCEAF (B), as assessed by WST-1 assay (A) and LDH assay (B). HDMEC were exposed for 24 h to different doses (0.01–100 µg/mL) of CCEAF, Triton X-100 as cytotoxic control or vehicle (control). Mean ± SEM (n = 4); *P < 0.05 vs. control.

2.5. Tube formation assay

A tube formation assay was performed to study the effect of CCEAF on the tube forming activity of HDMEC. In a first step, 50 µL growth factor-reduced Matrigel (Corning by VWR) was pipetted into each well of a 96-well plate and incubated for 30 min at 37 °C, resulting in the polymerization of the gel. Then, 1.5×10^4 HDMEC in ECGM-MV medium were added in each well and stimulated with 50 ng/mL vascular endothelial growth factor (VEGF, R&D Systems, Wiesbaden, Germany) in the presence or absence of 1 and 10 µg/mL CCEAF or vehicle. After 18 h culture at 37 °C, tube formation was observed using a phase-contrast microscope (BZ-8000; Keyence). The number of meshes, i.e. areas completely surrounded by endothelial tubes, was assessed by means of the Image J software with an angiogenesis analyzer plugin (National Institutes of Health (NIH), Bethesda, MD, USA). The experiments were performed in sextuplicate.

2.6. Spheroid sprouting assay

A spheroid sprouting assay was performed to study the effect of CCEAF on the sprouting activity of HDMEC. The cells were suspended in ECGM-MV medium containing 20% (w/v) methyl cellulose (Thermo Fischer Scientific, Dreieich, Germany) and seeded (500 cells/100 µL) in non-adherent round bottom 96-well plates (Greiner Bio-One, GmbH, Frickenhausen, Germany) for 24 h at 37 °C and 5% CO_2. These conditions guaranteed that all suspended cells per well contributed to the development of a single spheroid of defined size. The spheroids were then embedded in collagen gels. A collagen stock solution was prepared by mixing 8 vol of acidic collagen extract of rat tails (2 mg/mL, 4 °C; Serva Electrophoresis GmbH, Heidelberg, Germany) with 1 volume of 10 × M199 (Sigma-Aldrich) and 1 volume of 0.2 M NaOH to adjust the pH to 7.4. This stock solution was mixed in a 1:2 dilution with ECGM containing 20% FCS (Biochrom) and 0.5% (w/v) methyl cellulose to prevent sedimentation of the spheroids prior to the polymerization of the collagen gel. Then, 300 µL of the spheroid-containing gel (~150 spheroids/mL) was rapidly transferred into pre-warmed 24-well plates and allowed to polymerize for 45 min, after which 0.4 mL ECGM-MV containing 2 ng/mL VEGF (R&D Systems) and 1 and 10 µg/mL CCEAF or vehicle (DMSO; control) were pipetted on top of each gel. The gels were incubated at 37 °C and 5% CO_2 in a humidified atmosphere. After 24 h, spheroid sprouting was assessed by quantifying the cumulative sprout length, i.e. the overall length of all sprouts growing out of each spheroid, using a phase-contrast microscope (BZ-8000; Keyence). The analyses included 6–10 spheroids per experimental group.

2.7. Animals

The animal experiments were conducted in compliance with the German legislation on protection of animals and the NIH's Guide for the Care and Use of Laboratory Animals (Institute of Laboratory Animal Resources, National Research Council, Washington, DC, USA). They were approved by the local governmental animal protection committee (Saarland, Germany; permission number: 32/2015). The manuscript was prepared according to the ARRIVE guidelines for reporting experiments involving animals (McGrath et al., 2010).

We used 10- to 14-week-old female BALB/c mice (Institute for Clinical & Experimental Surgery, Homburg/Saar, Germany) exhibiting a body weight of 18–20 g. The mice were housed in groups of up to seven animals in a temperature-controlled environment with a relative humidity of 50–60% under a 12 h/12 h light-dark cycle. They had free access to pellet food (Altromin, Lage, Germany) and tap water.

Urine-soaked beddings from males were put into the cages of the female mice for the synchronization of their estrus cycles. The cycle stage of individual mice was assessed by cytological analysis of a vaginal lavage sample. For this purpose, 15 µL of 0.9% saline was carefully flushed into the vagina and subsequently pipetted onto a glass slide for the analysis under a phase-contrast microscope (CH-2; Olympus, Hamburg, Germany). To guarantee identical cycle stages of donor and recipient mice, only mice in the estrus stage served for the induction of endometriotic lesions.

2.8. Peritoneal endometriosis model

Uterine tissue samples from 7 donor mice were sutured to the peritoneal wall of recipient mice, as described previously (Rudzitis-Auth et al., 2012). For this purpose, the donor mice were anesthetized by an intraperitoneal (i.p.) injection of 75 mg/kg of ketamine (Ursotamin®; Serumwerke Bernburg, Bernburg, Germany) and 15 mg/kg of xylazin (Rompun®; Bayer, Leverkusen, Germany). After midline laparotomy, the two uterine horns were excised and transferred to a Petri dish that contained Dulbecco's modified Eagle medium (DMEM; PAN-Biotech, Aidenbach, Germany; 10% FCS, 100 U/mL penicillin, 0.1 mg/mL streptomycin; Biochrom). Then, the horns were cut open longitudinally with a micro scissors and 2 mm uterine tissue samples were removed with a dermal biopsy punch (Stiefel Laboratorium GmbH, Offenbach am Main, Germany). Two tissue samples were fixed with a

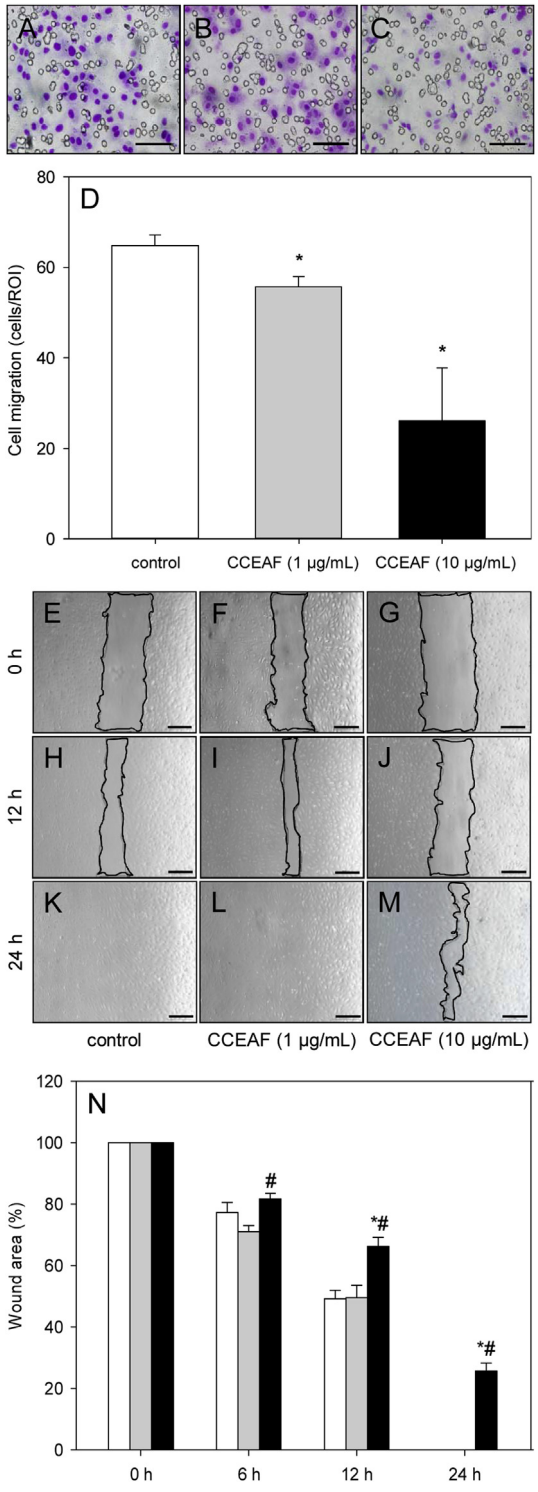

Fig. 2. Effects of CCEAF on migration of HDMEC. A–C: Light microscopic images of HDMEC after migration to the lower membrane surface of the transwell migration assay. Before the assay, the cells were exposed for 24 h to vehicle (A, control), 1 µg/mL (B) or 10 µg/mL CCEAF (C). Scale bars: 50 µm. D: Cell migration (cells/ROI) of HDMEC, which were exposed for 24 h to vehicle (control, white bar), 1 µg/mL CCEAF (gray bar) or 10 µg/mL CCEAF (black bar), as assessed by the transwell migration assay. Mean ± SEM (n = 4); *P < 0.05 vs. control. E–M: Phase-contrast microscopic images of HDMEC, which were exposed to vehicle (E, H, K, control), 1 µg/mL CCEAF (F, I, L) or 10 µg/mL CCEAF (G, J, M), at 0, 12 and 24 h after scratching. The black lines outline the wound areas. Scale bars: 160 µm. N: Wound area (% of 0 h) created by scratching HDMEC, which were exposed to vehicle (control, white bars), 1 µg/mL CCEAF (gray bars) or 10 µg/mL CCEAF (black bars), as assessed by the scratch wound healing assay. Mean ± SEM (n = 12–14); *P < 0.05 vs. control; #P < 0.05 vs. 1 µg/mL.

6–0 Prolene suture (Ethicon Products, Norderstedt, Germany) on each site of the abdominal wall of 22 anesthetized recipient mice through a midline incision. Finally, the laparotomy was closed with running 6–0 Prolene muscle and skin sutures.

After the surgical induction of endometriotic lesions, the recipient mice were divided into two groups by a third party investor using a randomly numbered table. The mice either received 50 mg/kg CCTE i.p. (dissolved in a combination of 3% DMSO and saline) (n = 12) or vehicle (control; n = 10) every other day. The treatment was started one day after the induction of endometriosis and continued throughout 4 weeks until the end of the experiments. The housing conditions for the animals and the time points of CCTE injection were identical in the two groups.

2.9. High-resolution ultrasound imaging and analysis

As described previously in detail (Laschke et al., 2010; Rudzitis-Auth et al., 2013), the endometriotic lesions were analyzed by means of high-resolution ultrasound imaging (Vevo 770™; VisualSonics, Toronto, ON, Canada) directly after surgical induction (day 0) as well as on day 7, 14, 21 and 28. The analyses included the quantification of the overall volume of the lesions, their stromal tissue and cysts (in mm^3). Based on these parameters, we additionally calculated the growth of the lesions and their stromal tissue (in % of the initial lesion and stromal tissue size) as well as the fraction of cyst-containing lesions (in % of all analyzed lesions).

After the last ultrasound imaging, the anesthetized mice were laparotomized and a digital caliper was used to assess the largest diameter (D1) and perpendicularly aligned diameter (D2) of the endometriotic lesions. The lesion size (S) was then calculated as follows: $S = D1 \times D2 \times \pi/4$ (Becker et al., 2008). Finally, the mice were sacrificed with an overdose of anesthetics and the endometriotic lesions were excised for additional histological and immunohistochemical analyses.

2.10. Histology and immunohistochemistry

The excised endometriotic lesions were fixed in formalin and embedded in paraffin to cut 3 µm-thick sections. To investigate the morphology of the lesions, sections were stained with hematoxylin and eosin (HE).

Additional sections were stained with a monoclonal rat anti-mouse antibody against the endothelial cell marker CD31 (1:300; Dianova, Hamburg, Germany) followed by a goat anti-rat IgG Alexa555 secondary antibody (Thermo Fisher Scientific). Hoechst 33342 (2 µg/mL; Sigma-Aldrich) served for nuclear staining. The sections were analyzed with a BZ-8000 microscope (Keyence) for the quantification of the microvessel density (given in mm^{-2}). For this purpose, the overall number of $CD31^+$ microvessels within an endometriotic lesion was counted and divided by the stromal lesion area.

Moreover, sections were stained with a rabbit polyclonal antibody against the proliferation marker Ki67 (1:500; Abcam, Cambridge, UK) and a rabbit polyclonal antibody against the apoptosis marker cleaved caspase (Casp)-3 (1:100; Cell Signaling Technology, Frankfurt, Germany) as primary antibodies followed by a biotinylated goat anti-rabbit IgG antibody (ready-to-use; Abcam). The biotinylated antibody was detected by peroxidase-labeled-streptavidin (ready-to-use; Abcam). 3-Amino-9-ethylcarbazole (Abcam) served as chromogen. The sections were counterstained with Mayer's hemalaun (Merck). The fraction of proliferating and apoptotic stromal and glandular cells (given in % of

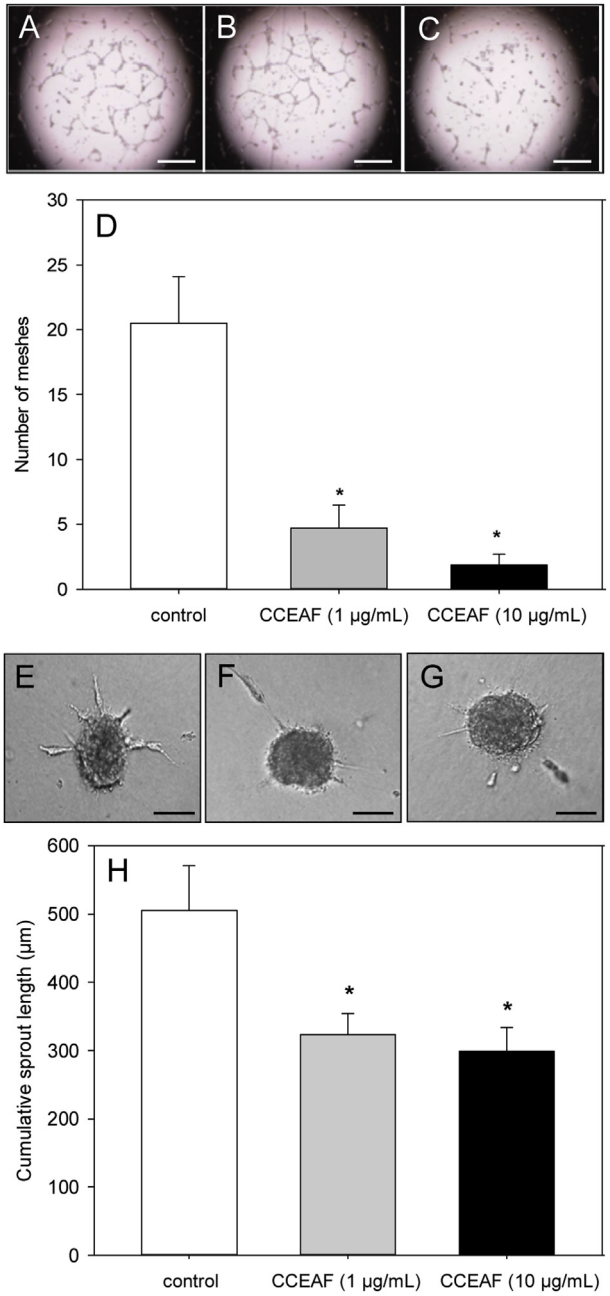

Fig. 3. Effects of CCEAF on tube formation and sprouting activity of HDMEC. A–C: Phase-contrast microscopic images of tube-forming HDMEC, which were exposed to vehicle (A, control), 1 µg/mL (B) or 10 µg/mL CCEAF (C). Scale bars: 740 µm. D: Number of meshes, i.e. areas completely surrounded by tube-forming HDMEC, which were exposed to vehicle (control, white bar), 1 µg/mL CCEAF (gray bar) or 10 µg/mL CCEAF (black bar), as assessed by the tube formation assay. Mean ± SEM (n = 6); *P < 0.05 vs. control. E–G: Phase-contrast microscopic images of sprouting HDMEC spheroids, which were exposed to vehicle (E, control), 1 µg/mL CCEAF (F) or 10 µg/mL CCEAF (G). Scale bars: 95 µm. H: Cumulative sprout length (µm) of HDMEC spheroids, which were exposed to vehicle (control, white bar), 1 µg/mL CCEAF (gray bar) or 10 µg/mL CCEAF (black bar), as assessed by the spheroid sprouting assay. Mean ± SEM (n = 6–10); *P < 0.05 vs. control.

all analyzed cells) was evaluated by means of a BX-60 microscope (Olympus).

For the immunohistochemical detection of $CD68^+$ macrophages, myeloperoxidase $(MPO)^+$ neutrophilic granulocytes and $CD3^+$ lymphocytes, sections were incubated with a rabbit polyclonal anti-CD68 antibody (1:50; Abcam), a rabbit polyclonal anti-MPO antibody (1:100; Abcam) and a rabbit polyclonal anti-CD3 antibody (1:100; Abcam) as primary antibodies followed by the secondary antibody as described above. The numbers of the different immune cell types (given in mm^2 stromal lesion area) were counted in 4 randomized ROIs per lesion.

2.11. Statistics

Data were first tested for normal distribution and equal variance. Differences between two groups were assessed by the unpaired Student's t-test (parametric data) or by the Mann-Whitney rank sum test (non-parametric data). Differences between multiple groups were assessed by analysis of variance (ANOVA) followed by the Student-Newman-Keuls test. To test for time effects within each experimental group, ANOVA for repeated measurements followed by the Student-Newman-Keuls test was applied (SigmaPlot 12.5; Jandel Corporation, San Rafael, CA). All data are given as mean ± SEM. Statistical significance was accepted for a value of $P < 0.05$.

3. Results

3.1. CCEAF effect on endothelial cell viability

In a first step, we analyzed the effect of different doses of CCEAF on the viability of HDMEC using the WST-1 assay. We found that there was no toxic effect of CCEAF between 0.01 and 10 µg/mL, whereas doses of 50 and 100 µg/mL significantly reduced the viability of the exposed cells (Fig. 1A). These results were confirmed in the LDH assay (Fig. 1B). Based on these data we used the non-toxic doses of 1 and 10 µg/mL CCEAF in all further *in vitro* experiments to investigate the effect of the plant extract on different endothelial cell functions.

3.2. CCEAF effect on endothelial cell migration

We next performed a transwell migration assay and a scratch wound healing assay to analyze the effect of CCEAF on the migration of HDMEC. In the transwell migration assay, 1 and 10 µg/mL CCEAF significantly diminished the migration of HDMEC when compared to vehicle-treated controls (Fig. 2A–D). In addition, identical doses of the plant extract significantly delayed the closure of scratched wounds in a dose-dependent manner (Fig. 2E-N).

3.3. CCEAF effect on endothelial tube and sprout formation

In a final set of *in vitro* experiments, we performed a tube formation assay and a spheroid sprouting assay. In line with our previous results, we found that 1 and 10 µg/mL CCEAF markedly suppresses endothelial cell tube formation (Fig. 3A–D). Moreover, CCEAF suppressed the sprouting activity of HDMEC, as indicated by a significantly reduced cumulative sprout length of CCEAF-treated HDMEC spheroids when compared to vehicle-treated controls (Fig. 3E–H).

3.4. CCTE effects on developing endometriotic lesions

Based on our promising *in vitro* results demonstrating a substantial anti-angiogenic action of CCEAF, we next analyzed the effects of the plant extract on growth, cyst formation, vascularization and immune cell infiltration of endometriotic lesions in mice. The animals tolerated the treatment with the extract well, as indicated by normal feeding, cleaning and sleeping habits, which did not differ from those of vehicle-treated controls. Endometriotic lesions were induced by transplantation of uterine tissue samples from donor animals to the wall of the peritoneal cavity in recipient mice. Throughout the 4-week experiment, the uterine tissue samples developed into endometriotic lesions with cyst-like dilated endometrial glands and an endometrial stroma, which could be clearly differentiated from the surrounding tissue using high-

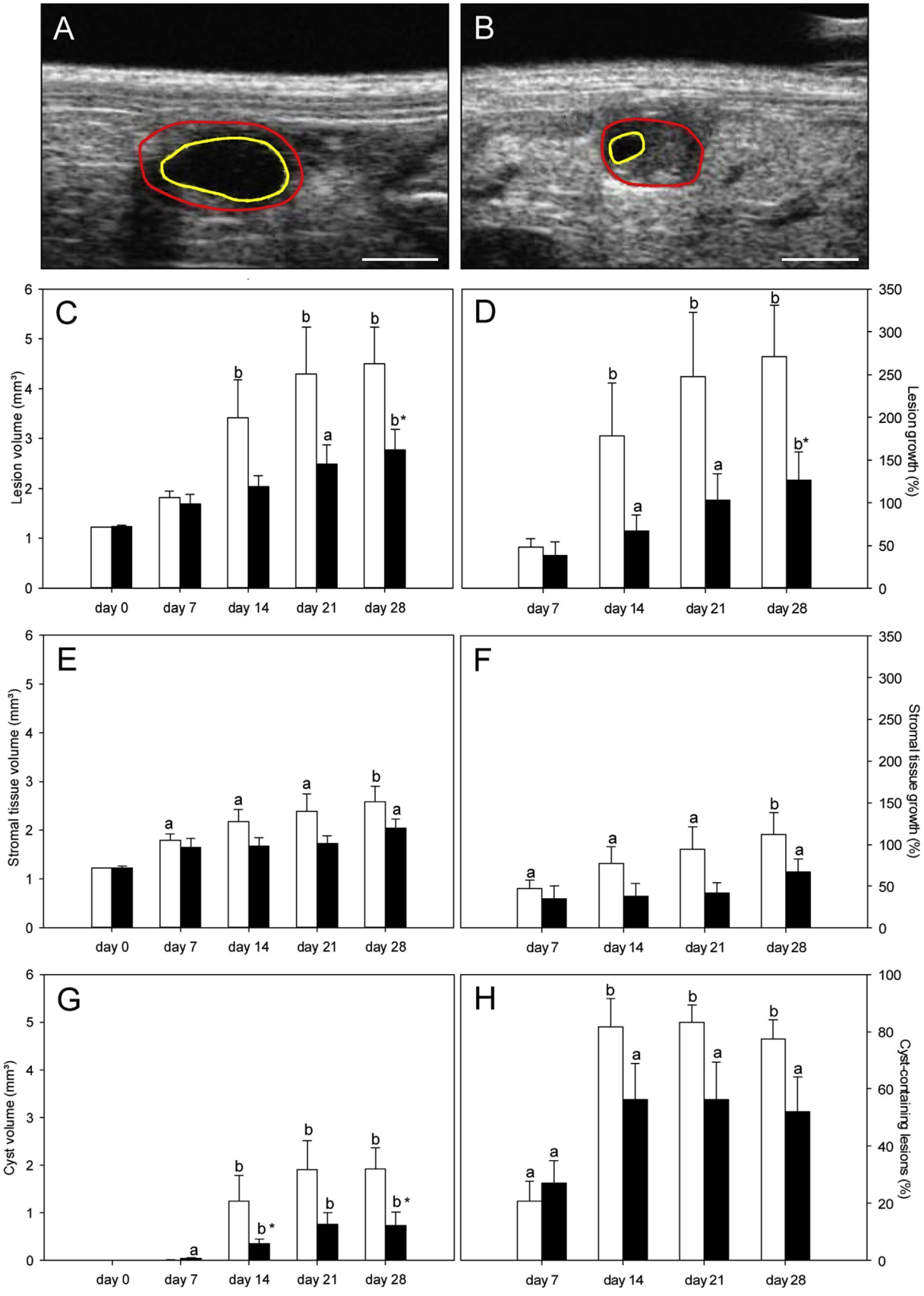

(caption on next page)

Fig. 4. Effects of CCTE on growth and cyst formation of endometriotic lesions. A, B: High-resolution ultrasound imaging of developing endometriotic lesions (borders marked by red line, cysts marked by yellow line) 28 days after transplantation of uterine tissue samples to the abdominal wall of BALB/c mice. The animals received either vehicle (A) or 50 mg/kg CCTE i.p. (B). Scale bars: 1.4 mm. C–H: Overall lesion volume (C, mm^3), lesion growth (D, %), stromal tissue volume (E, mm^3), stromal tissue growth (F, %), cyst volume (G, mm^3) and fraction of cyst-containing lesions (H, %) of BALB/c mice, which received either vehicle (control, white bars) or 50 mg/kg CCTE i.p. (black bars), as assessed by high-resolution ultrasound imaging throughout an observation period of 28 days. Mean ± SEM (n = 10–12); *P < 0.05 vs. control; ^{a}P < 0.05 vs. day 0; ^{b}P < 0.05 vs. day 0 and 7. (For interpretation of the references to colour in this figure legend, the reader is referred to the Web version of this article.)

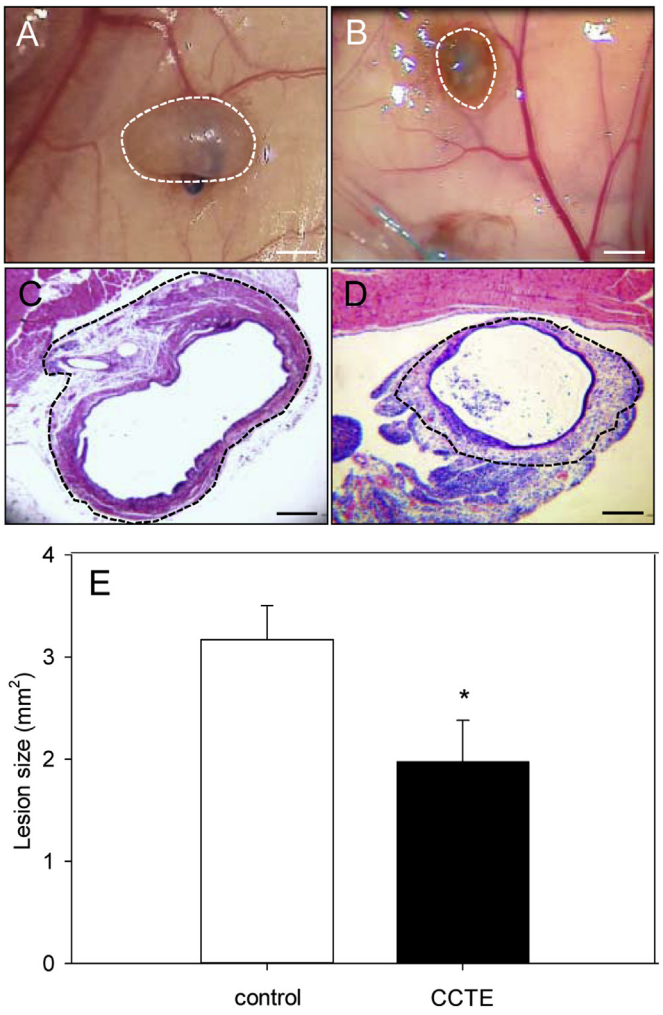

Fig. 5. Effects of CCTE on size and histomorphology of endometriotic lesions. A, B: Macroscopic appearance of endometriotic lesions (borders marked by broken line) 28 days after transplantation of uterine tissue samples to the abdominal wall of BALB/c mice. The animals received either vehicle (A) or 50 mg/kg CCTE i.p. (B). Scale bars: 750 µm. C, D: HE-stained endometriotic lesions (borders marked by broken line) 28 days after transplantation of uterine tissue samples to the abdominal wall of BALB/c mice. The animals received either vehicle (C) or 50 mg/kg CCTE i.p. (D). Scale bars: 270 µm. E: Size (mm^2) of endometriotic lesions of BALB/c mice, which received either vehicle (control, white bar) or 50 mg/kg CCTE i.p. (black bar), as assessed by caliper measurement on day 28. Mean ± SEM (n = 10–12); *P < 0.05 vs. control.

resolution ultrasound imaging (Fig. 4A and B). High-resolution ultrasound imaging demonstrated that the uterine tissue samples exhibited a comparable initial size of ~1.2 mm^3 in CCTE- and vehicle-treated mice, providing standardized starting conditions for further analyses of their growth and cyst formation (Fig. 4C). Of interest, the process of development into endometriotic lesions was markedly inhibited in CCTE-treated animals. Their lesions exhibited a significantly reduced volume and growth rate on day 28 when compared to controls (Fig. 4C and D). This was due to a lower stromal and cyst volume (Fig. 4E–G). Moreover, the fraction of cyst-containing lesions was also slightly decreased in CCTE-treated mice (Fig. 4H).

These findings were further confirmed by caliper measurements and HE-stainings of the lesions on day 28 (Fig. 5A–E). As expected, CCTE-treated lesions exhibited a smaller size (Fig. 5B and E) and also contained smaller cyst-like dilated glands (Fig. 5D) when compared to vehicle-treated controls (Fig. 5A, C and E).

Additional immunohistochemical analyses revealed that CCTE-treated endometriotic lesions exhibited a significantly lower density of $CD31^+$ microvessels when compared to vehicle-treated controls (Fig. 6A–C). Of note, we did not detect any Casp-3^+ apoptotic cells within the lesions of both groups on day 28. Therefore, we assumed that the observed differences in lesion sizes were primarily caused by a reduced cell proliferation in CCTE-treated animals. In line with this view, we found that CCTE-treated lesions contained less proliferating $Ki67^+$ stromal cells, whereas the number of proliferating glandular cells was almost comparable in the two groups (Fig. 6D–F).

To assess potential anti-inflammatory effects of CCTE, we finally analyzed the immune cell infiltration within the endometriotic lesions (Fig. 7A–I). We found that lesions in CCTE-treated mice were infiltrated by significantly lower numbers of $CD68^+$ macrophages (Fig. 7A, D and G) and $CD3^+$ lymphocytes (Fig. 7C, F and I) when compared to vehicle-treated controls. In contrast, the numbers of infiltrating MPO^+ neutrophilic granulocytes did not differ between the two groups (Fig. 7B, E and H).

4. Discussion

Calligonum comosum is a herb, which exhibits anti-inflammatory (Liu et al., 2001; Abdallah et al., 2014), anti-bacterial (Hammami et al., 2011; Alkhalifah, 2013), anti-oxidant (Badria et al., 2007) and anti-cancer activity (Badria et al., 2007; Abdo et al., 2015). In the present study, we now demonstrate for the first time that *Calligonum comosum* is also effective in inhibiting angiogenesis. This pleiotropic action profile makes it a promising candidate for the treatment of endometriosis. Accordingly, we found that CCTE suppresses the growth, cyst formation, vascularization and immune cell infiltration of murine endometriotic lesions. These effects may be mediated by several active phytochemical components in CCTE, such as flavonoids (quercetin, kaempferols and catechins) and polyphenols (tannins) (EI Sayyad and Wagner, 1978; Ahmed et al., 2016; Cheruth et al., 2016).

Based on viability and cytotoxicity assays, we herein used non-toxic doses of 1 and 10 µg/mL CCEAF for our *in vitro* experiments. These doses effectively inhibited cell migration, tube formation and sprouting of HDMEC, indicating that CCEAF targets multiple steps of the angiogenic process. This is an interesting observation given the fact that individual components of *Calligonum comosum* have been shown to promote the formation of new blood vessels. For instance, Tulio et al. (2012) reported that polyphenols like tannins stimulate the migration and tube formation of human umbilical vein endothelial cells (HUVEC) by activation of PI3K/Akt/eNOS signaling. β-Sitosterol (BS), another active component of *Calligonum comosum*, has also been shown to promote angiogenesis and, thus, to be beneficial for wound healing (Moon et al., 1999). These contradictory findings may be explained by the fact that *Calligonum comosum* contains various phytochemical compounds. Their mixture and resulting concentration profiles may simultaneously activate or suppress multiple intracellular pathways and

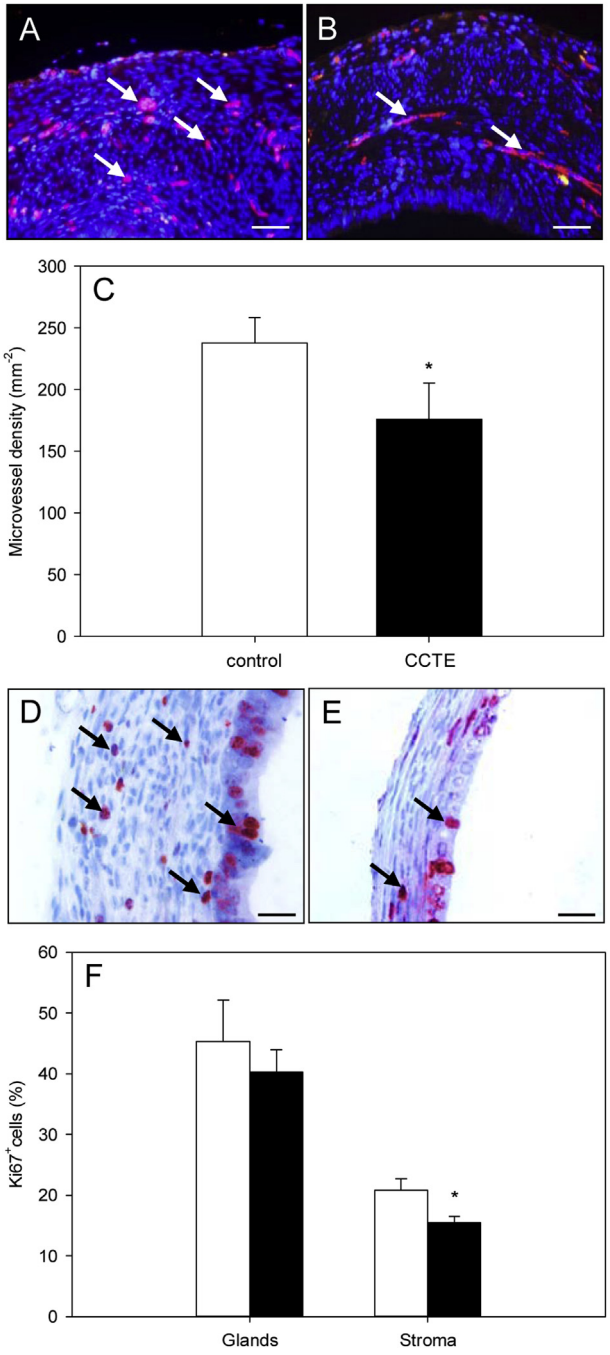

Fig. 6. Effects of CCTE on vascularization and proliferation of endometriotic lesions. A, B: Immunofluorescent detection of microvessels (arrows) within endometriotic lesions 28 days after transplantation of uterine tissue samples to the abdominal wall of BALB/c mice. The animals received either vehicle (A) or 50 mg/kg CCTE i.p. (B). Sections were stained with Hoechst 33342 to identify cell nuclei (blue) and an antibody against CD31 for the detection of microvascular endothelial cells (red). Scale bars: 50 µm. C: Microvessel density (mm^{-2}) of endometriotic lesions of BALB/c mice, which received either vehicle (control, white bar) or 50 mg/kg CCTE i.p. (black bar), as assessed by immunohistochemistry on day 28. Mean ± SEM (n = 8–10); *P < 0.05 vs. control. D, E: Immunohistochemical detection of Ki67$^+$ proliferating cells (arrows) within endometriotic lesions 28 days after transplantation of uterine tissue samples to the abdominal wall of BALB/c mice. The animals received either vehicle (D) or 50 mg/kg CCTE i.p. (E). Scale bars: 50 µm. F: Ki67$^+$ cells (%) within the glands and the stroma of endometriotic lesions of BALB/c mice, which received either vehicle (control, white bars) or 50 mg/kg CCTE i.p. (black bars), as assessed by immunohistochemistry on day 28. Mean ± SEM (n = 8–10); *P < 0.05 vs. control.

finally induce specific inhibitory effects on endothelial cells, which completely differ from those of individual compounds. This point of view needs further clarification in future studies, unraveling the complex network of molecular signaling that is activated by *Calligonum comosum* in endothelial cells.

In the present study, we surgically induced endometriotic lesions by transplantation of uterine tissue samples from syngeneic donor mice to the wall of the peritoneal cavity in recipient animals (Laschke et al., 2010). This approach does not mimic the clinical situation, where peritoneal endometriosis is assumed to be caused by retrograde menstruation of shed endometrial fragments from the uterine cavity (Sampson, 1927). Therefore, we only used mice in the estrus stage as donors and recipients for the induction of endometriosis to exclude differences between individual animals related to different sex hormone levels. An alternative model would have been the transplantation of tissue samples from one uterine horn into the peritoneal cavity of the identical animal (Pelch et al., 2012; Kiani et al., 2018). However, in this autologous model the harvesting of the uterine horn is associated with additional surgical trauma and increased levels of pro-inflammatory factors in the abdomen, such as tumor necrosis factor (TNF)-α and interleukin (IL)-6, which may influence the development of endometriotic lesions (Oral et al., 1996). In contrast, our syngeneic approach bears the advantage of a shorter surgical intervention and less trauma for the recipient animal and, thus, a better preservation of the physiological environment within the peritoneal cavity (Körbel et al., 2010). To analyze the effect of CCTE on murine endometriotic lesions, we chose a dose of 50 mg/kg body weight. In a previous *in vivo* toxicity study this dose has been shown to be safe (Kiani et al., 2016). Accordingly, the mice tolerated the treatment with CCTE well and their behaviour did not differ from that of control animals throughout the observation period of 4 weeks.

Our ultrasound analyses and caliper measurements revealed that CCTE significantly inhibits the growth of newly developing endometriotic lesions. This was not only due to a suppressed stromal tissue growth but also due to a markedly reduced volume of the cyst-like dilated endometrial glands within the lesions. The latter observation indicates that CCTE seems to affect the secretory activity of the glandular epithelium. Moreover, CCTE effectively deteriorated the lesions' vascularization in line with our *in vitro* results. This is an important finding, because angiogenesis is a major hallmark in the pathogenesis of endometriosis (Laschke and Menger, 2018). Particularly in early stages of the disease, blood vessel formation is a major prerequisite for the survival and proliferation of ectopic endometrial tissue inside the peritoneal cavity (May and Becker, 2008). Accordingly, we also detected a significantly reduced number of proliferating Ki67$^+$ cells in the stroma of CCTE-treated lesions when compared to controls.

The anti-angiogenic action of CCTE may be attributed to its high quercetin concentration, as measured in previous HPLC analyses (Kiani et al., 2016). In fact, quercetin suppresses angiogenesis by inhibition of cyclooxygenase (COX)-2 and lipoxygenase (LOX)-5 (Sagar et al., 2006; Seo et al., 2013). Moreover, it targets epidermal growth factor (EGF) receptor, human EGF receptor-2 (HER-2) and NFκB signaling (Zhao et al., 2014). Zhao et al. (2014) further showed that quercetin downregulates the expression of VEGFR-2. Besides quercetin, BS is also detected in high concentrations in CCTE (Kiani et al., 2016). BS interferes with multiple signaling pathways, which regulate cell cycle, proliferation, apoptosis, invasion, angiogenesis and inflammation (Bin Sayeed and Ameen, 2015). Of interest, Baskar et al. (2010) reported that BS exerts anti-cancer effects by increasing first apoptosis signal (FAS) levels and caspase-8 activity. However, in the present study we did not detect increased numbers of Casp-3$^+$ cells within CCTE-treated lesions. Hence, we suggest that the growth suppressive effect of the plant extract on endometriotic lesions is rather mediated by the inhibition of angiogenesis and cell proliferation than the induction of apoptotic cell death.

In addition to angiogenesis, inflammatory processes are crucially

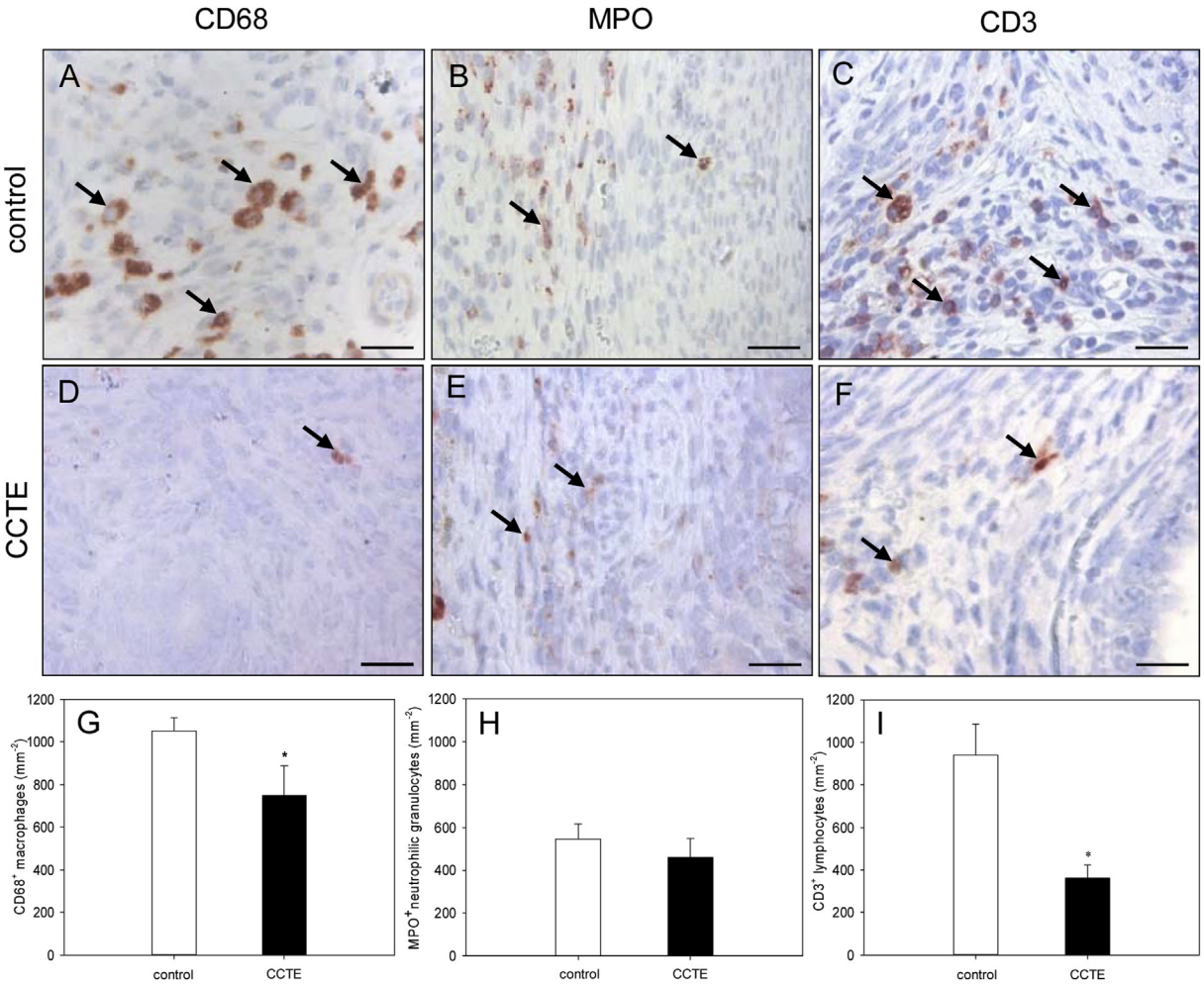

Fig. 7. Effects of CCTE on immune cell infiltration into endometriotic lesions. A–F: Immunohistochemical detection of $CD68^+$ macrophages (arrows, A, D), MPO^+ neutrophilic granulocytes (arrows, B, E) and $CD3^+$ lymphocytes (arrows, C, F) within endometriotic lesions 28 days after transplantation of uterine tissue samples to the abdominal wall of BALB/c mice. The animals received either vehicle (A–C) or 50 mg/kg CCTE i.p. (D–F). Scale bars: 30 µm. G–I: $CD68^+$ macrophages (G, mm^{-2}), MPO^+ neutrophilic granulocytes (H, mm^{-2}) and $CD3^+$ lymphocytes (I, mm^{-2}) within endometriotic lesions of BALB/c mice, which received either vehicle (control, white bars) or 50 mg/kg CCTE i.p. (black bars), as assessed by immunohistochemistry on day 28. Mean ± SEM (n = 8–10); *P < 0.05 vs. control.

involved in the pathogenesis of endometriosis (Jiang et al., 2016). Recent studies even indicate that endometriotic lesions induce a pro-inflammatory environment in the peritoneal cavity that plays a major role in the development of endometriosis-associated pain (McKinnon et al., 2015). In light of these important findings, we herein provide the first evidence that CCTE is also capable of suppressing immune cell infiltration into endometriotic lesions. This is most probably due to the well-known anti-inflammatory action of its flavonoid components (Abdel-Sattar et al., 2014). Treatment with CCTE particularly reduced the number of $CD3^+$ lymphocytes, which represent the main population of immune cells in rodent and human endometriotic lesions (Oosterlynck et al., 1993; Nenicu et al., 2014). In addition, we detected significantly lower numbers of $CD68^+$ macrophages in CCTE-treated lesions when compared to controls. The accumulation of active macrophages and their products plays an important role in the development of endometriotic lesions. The secretion of IL-6 and TNF-α by active peritoneal macrophages increases the aromatase activity of endometriotic stromal cells and the production of estrogen, the major hormonal trigger for the development of endometriotic lesions (Velasco et al., 2006). Macrophages also produce several pro-angiogenic factors, such as fibroblast growth factor (FGF), angiotensin and VEGF (Sunderkötter et al., 1994; McLaren et al., 1996), which stimulate the formation of new blood vessels in endometrial tissue (Lin et al., 2006).

5. Conclusions

We could demonstrate that CCEAF is a potent inhibitor of angiogenesis. Moreover, CCTE suppresses the growth, cyst formation, vascularization and immune cell infiltration of endometriotic lesions. Accordingly, *Calligonum comosum* extract, which is applied in traditional folkloric medicine for the treatment of various diseases, may represent a promising dietary candidate for the prevention and therapy of endometriosis.

Author contributions

Kiandokht Kiani performed experiments, analyzed data, wrote the manuscript, revised and approved the final manuscript version (kiani.kiandokht@gmail.com).

Jeannette Rudzitis-Auth performed experiments, analyzed data, revised and approved the final manuscript version (jeannette.rudzitis-auth@uks.eu). Claudia Scheuer performed experiments, analyzed data, revised and approved the final manuscript version (claudia.scheuer@uks.eu). Mansoureh Movahedin designed the study, revised and approved the final manuscript version (movahed.m@modares.ac.ir). Seyede Nargess Sadati Lamardi performed extract preparations and analyses, revised and approved the final manuscript version (n_sadati@tums.ac.ir). Hossein Malekafzali Ardakani designed the study, revised

and approved the final manuscript version (malek179@gmail.com). Vivien Becker performed experiments, analyzed data, revised and approved the final manuscript version (vivien.becker@uks.eu). Ashraf Moini designed the study, revised and approved the final manuscript version (a_moini@royaninstitute.org). Reza Aflatoonian designed the study, revised and approved the final manuscript version (r.aflatoonian@gmail.com).

Seyed Nasser Ostad performed experiments, analyzed data, revised and approved the final manuscript version (ostadnas@tums.ac.ir). Michael D. Menger designed the study, revised and approved the final manuscript version (michael.menger@uks.eu).

Matthias W. Laschke designed the study, wrote the manuscript, revised and approved the final manuscript version (matthias.laschke@uks.eu).

Conflict of interest

The authors declare that they have no conflicts of interest.

Funding

This study was supported by the Saarland University, Germany, the Tehran University of Medical Sciences, Iran National Science Foundation and Royan Institute for Reproductive Biomedicine, ACECR, Tehran, Iran.

Acknowledgements

We are grateful for the excellent technical assistance of Janine Becker, Caroline Bickelmann, Christina Marx, Ruth M. Nickels and Julia Parakenings (Institute for Clinical & Experimental Surgery, Homburg/Saar). This article is extracted from the Ph.D. thesis of Kiandokht Kiani.

Appendix A. Supplementary data

Supplementary data to this article can be found online at https://doi.org/10.1016/j.jep.2019.111918.

Glossary

ANOVA	analysis of variance
Casp	cleaved caspase
CCEAF	*Calligonum comosum* ethyl acetate fraction
CCTE	*Calligonum comosum* total extract
COX	cyclooxygenase
DMSO	dimethyl sulfoxide
EGF	epidermal growth factor
FAS	first apoptosis signal
FCS	fetal calf serum
FGF	fibroblast growth factor
HDMEC	human dermal microvascular endothelial cells
HE	hematoxylin and eosin
HUVEC	human umbilical vein endothelial cells
IL	interleukin
LDH	lactate dehydrogenase
LOX	lipoxygenase
MPO	myeloperoxidase
PBS	phosphate-buffered saline
ROIs	regions of interest
TNF	tumor necrosis factor
VEGF	vascular endothelial growth factor
WST-1	water-soluble tetrazolium

References

Abdallah, H.M.I., Asaad, G.F., Arbid, M.S., Abdel-Sattar, E.A., 2014. Anti-inflammatory, antinociceptive, antipyretic and gastroprotective effects of calligonum comosum in rats and mice. IJTPR 6, 26–33.

Abdel-Sattar, E.A., Mouneir, S.M., Asaad, G.F., Abdallah, H.M., 2014. Protective effect of Calligonum comosum on haloperidol-induced oxidative stress in rat. Toxicol. Ind. Health 30, 147–153.

Abdo, W., Hirata, A., Shukry, M., Kamal, T., Abdel-Sattar, E., Mahrous, E., Yanai, T., 2015. Calligonum comosum extract inhibits diethylnitrosamine-induced hepatocarcinogenesis in rats. Oncol. Lett. 10, 716–722.

Adamson, G.D., 2011. Endometriosis classification: an update. Curr. Opin. Obstet. Gynecol. 23, 213–220.

Ahmed, H., Moawad, A., Owis, A., AbouZid, S., Ahmed, O., 2016. Flavonoids of Calligonum polygonoides and their cytotoxicity. Pharm. Biol. 54, 2119–2126.

Ali, R., Mirza, Z., Ashraf, G.M., Kamal, M.A., Ansari, S.A., Damanhouri, G.A., Abuzenadah, A.M., Chaudhary, A.G., Sheikh, I.A., 2012. New anticancer agents: recent developments in tumor therapy. Anticancer Res. 32, 2999–3005.

Alkhalifah, D.H.M., 2013. In-vitro antibacterial activity of ethanol extract of *Calligonum comosum* plant against four human pathogens in Saudi Arabia. Int. J. Pl. An. Env. Sci. 3, 170–175.

Alwakeel, S.S., 2008. Microbial and heavy metals contamination of herbal medicines. Res. J. Microbiol. 3, 683–691.

Badria, F.A., Ameen, M., Akl, M.R., 2007. Evaluation of cytotoxic compounds from calligonum comosum L. growing in Egypt. Z. Naturforsch. C 62, 656–660.

Baskar, A.A., Ignacimuthu, S., Paulraj, G.M., Al Numair, K.S., 2010. Chemopreventive potential of beta-Sitosterol in experimental colon cancer model–an in vitro and in vivo study. BMC Complement Altern. Med. 10, 24.

Becker, C.M., Rohwer, N., Funakoshi, T., Cramer, T., Bernhardt, W., Birsner, A., Folkman, J., D'Amato, R.J., 2008. 2-methoxyestradiol inhibits hypoxia-inducible factor-1{alpha} and suppresses growth of lesions in a mouse model of endometriosis. Am. J. Pathol. 172, 534–544.

Bin Sayeed, M.S., Ameen, S.S., 2015. Beta-Sitosterol: a promising but orphan nutraceutical to fight against cancer. Nutr. Canc. 67, 1214–1220.

Burney, R.O., Giudice, L.C., 2012. Pathogenesis and pathophysiology of endometriosis. Fertil. Steril. 98, 511–519.

Cheong, Y., Tay, P., Luk, F., Gan, H.C., Li, T.C., Cooke, I., 2008. Laparoscopic surgery for endometriosis: how often do we need to re-operate? J. Obstet. Gynaecol. 28, 82–85.

Cheruth, A.J., Al Naqbi, K.M.A., El-Kaabi, A.A.A.S., Odeh, O.W.Y., Kandhan, K., Maqsood, S., Kurup, S.S., Sakkir, S., 2016. In vitro antioxidant activities and screening of phytochemicals from methanolic and ethyl acetate extracts of Calligonum comosum L'Her. Orient. Pharm. Exp. Med. 16, 209–215.

Crosignani, P., Olive, D., Bergqvist, A., Luciano, A., 2006. Advances in the management of endometriosis: an update for clinicians. Hum. Reprod. Update 12, 179–189.

El Sayyad, S., Wagner, H., 1978. A phytochemical study of Calligonum comosum L. Henry. Planta Med. 33, 262–264.

El-Hawary, Z.M., Kholief, T.S., 1990. Biochemical studies on some hypoglycemic agents (II) effect of Calligonum comosum extract. Arch Pharm. Res. (Seoul) 13, 113–116.

Giudice, L.C., Kao, L.C., 2004. Endometriosis. Lancet 364, 1789–1799.

Hammami, R., Farhat, I., Zouhir, A., Fedhila, S., 2011. Detection and extraction of anti-Listerial compounds from Calligonum comosum, a medicinal plant from arid regions of Tunisia. Afr. J. Tradit., Complementary Altern. Med. 8, 322–327.

Jiang, L., Yan, Y., Liu, Z., Wang, Y., 2016. Inflammation and endometriosis. Front. Biosci. (Online) 21, 941–948.

Jiang, Q.Y., Wu, R.J., 2012. Growth mechanisms of endometriotic cells in implanted places: a review. Gynecol. Endocrinol. 28, 562–567.

Kiani, K., Movahedin, M., Malekafzali, H., Mirfasihi, F., Sadati, S.N., Moini, A., Ostad, S., Aflatoonian, R., 2018. Effect of the estrus cycle stage on the establishment of murine endometriosis lesions. Int. J. Reprod. Biomed. (Yazd) 16, 305–314.

Kiani, K., Sadati Lamardi, S.N., Ostad, S.N., Malekafzali Ardakani, H., Batooli, H., Movahedin, M., Aflatoonian, R., Moini, A., 2016. Quantification of quercetin, catechin, and βsitosterol, antioxidant and acute toxic effects of calligonum comosum L' Her different parts extract. Int. J. Adv. Res. 4, 380–388.

Körbel, C., Menger, M.D., Laschke, M.W., 2010. Size and spatial orientation of uterine tissue transplants on the peritoneum crucially determine the growth and cyst formation of endometriosis-like lesions in mice. Hum. Reprod. 25, 2551–2558.

Laschke, M.W., Körbel, C., Rudzitis-Auth, J., Gashaw, I., Reinhardt, M., Hauff, P., Zollner, T.M., Menger, M.D., 2010. High-resolution ultrasound imaging: a novel technique for the noninvasive in vivo analysis of endometriotic lesion and cyst formation in small animal models. Am. J. Pathol. 176, 585–593.

Laschke, M.W., Menger, M.D., 2012. Anti-angiogenic treatment strategies for the therapy of endometriosis. Hum. Reprod. Update 18, 682–702.

Laschke, M.W., Menger, M.D., 2018. Basic mechanisms of vascularization in endometriosis and their clinical implications. Hum. Reprod. Update 24, 207–224.

Lin, Y.J., Lai, M.D., Lei, H.Y., Wing, L.Y., 2006. Neutrophils and macrophages promote angiogenesis in the early stage of endometriosis in a mouse model. Endocrinology 147, 1278–1286.

Liu, X.M., Zakaria, M.N., Islam, M.W., Radhakrishnan, R., Ismail, A., Chen, H.B., Chan, K., Al-Attas, A., 2001. Anti-inflammatory and anti-ulcer activity of Calligonum comosum in rats. Fitoterapia 72, 487–491.

May, K., Becker, C.M., 2008. Endometriosis and angiogenesis. Minerva Ginecol. 60, 245–254.

McGrath, J.C., Drummond, G.B., McLachlan, E.M., Kilkenny, C., Wainwright, C.L., 2010. Guidelines for reporting experiments involving animals: the ARRIVE guidelines. Br. J. Pharmacol. 160, 1573–1576.

McKinnon, B.D., Bertschi, D., Bersinger, N.A., Mueller, M.D., 2015. Inflammation and nerve fiber interaction in endometriotic pain. Trends Endocrinol. Metabol. 26, 1–10.

McLaren, J., Prentice, A., Charnock-Jones, D.S., Millican, S.A., Müller, K.H., Sharkey, A.M., Smith, S.K., 1996. Vascular endothelial growth factor is produced by peritoneal

fluid macrophages in endometriosis and is regulated by ovarian steroids. J. Clin. Investig. 98, 482–489.
Moon, E.J., Lee, Y.M., Lee, O.H., Lee, M.J., Lee, S.K., Chung, M.H., Park, Y.I., Sung, C.K., Choi, J.S., Kim, K.W., 1999. A novel angiogenic factor derived from Aloe vera gel: beta-sitosterol, a plant sterol. Angiogenesis 3, 117–123.
Nenicu, A., Körbel, C., Gu, Y., Menger, M.D., Laschke, M.W., 2014. Combined blockade of angiotensin II type 1 receptor and activation of peroxisome proliferator-activated receptor-γ by telmisartan effectively inhibits vascularization and growth of murine endometriosis-like lesions. Hum. Reprod. 29, 1011–1024.
Oosterlynck, D.J., Cornillie, F.J., Waer, M., Koninckx, P.R., 1993. Immunohistochemical characterization of leucocyte subpopulations in endometriotic lesions. Arch. Gynecol. Obstet. 253, 197–206.
Oral, E., Olive, D.L., Arici, A., 1996. The peritoneal environment in endometriosis. Hum. Reprod. Update 2, 385–398.
Pelch, K.E., Sharpe-Timms, K.L., Nagel, S.C., 2012. Mouse model of surgically-induced endometriosis by auto-transplantation of uterine tissue. JoVE 59, e3396.
Ranjbarfordoei, A., Vandamme, P., Samson, R., 2013. Some ecophysiological characteristics of artà (Calligonum comosum L' Hérit) in response to drought stress. For. Sci. Prac. 15, 114–120.
Ricci, A.G., Olivares, C.N., Bilotas, M.A., Bastón, J.I., Singla, J.J., Meresman, G.F., Barañao, R.I., 2013. Natural therapies assessment for the treatment of endometriosis. Hum. Reprod. 28, 178–188.
Rudzitis-Auth, J., Körbel, C., Scheuer, C., Menger, M.D., Laschke, M.W., 2012. Xanthohumol inhibits growth and vascularization of developing endometriotic lesions. Hum. Reprod. 27, 1735–1744.
Rudzitis-Auth, J., Menger, M.D., Laschke, M.W., 2013. Resveratrol is a potent inhibitor of vascularization and cell proliferation in experimental endometriosis. Hum. Reprod. 28, 1339–1347.
Sagar, S.M., Yance, D., Wong, R.K., 2006. Natural health products that inhibit angiogenesis: a potential source for investigational new agents to treat cancer-Part 1. Curr. Oncol. 13, 14–26.
Samejo, M.Q., Memon, S., Bhanger, M.I., Khan, K.M., 2011. Preliminary phytochemicals screening of Calligonum polygonoides Linn. J. Pharm. Res. 4, 4402–4403.
Sampson, J.A., 1927. Peritoneal endometriosis due to menstrual dissemination of endometrial tissues into the peritoneal cavity. Am. J. Obstet. Gynecol. 14, 422–469.
Scutiero, G., Iannone, P., Bernardi, G., Bonaccorsi, G., Spadaro, S., Volta, C.A., Greco, P., Nappi, L., 2017. Oxidative stress and endometriosis: a systematic review of the literature. Oxid. Med. Cell. Longev., 7265238 2017.
Seo, E.J., Kuete, V., Kadioglu, O., Krusche, B., Schröder, S., Greten, H.J., Arend, J., Lee, I.S., Efferth, T., 2013. Antiangiogenic activity and pharmacogenomics of medicinal plants from traditional Korean medicine. Evid. Based. Complement. Alternat. Med. 2013, 131306.
Sunderkötter, C., Steinbrink, K., Goebeler, M., Bhardwaj, R., Sorg, C., 1994. Macrophages and angiogenesis. J. Leukoc. Biol. 55, 410–422.
Tahmasebi, F., Movahedin, M., Mazaheri, Z., 2018. Antioxidant effects of calligonum extract on ovarian tissue of PCO model: an experimental study. Int. J. Reprod. Biomed. (Yazd). 16, 641–648.
Tulio Jr., A.Z., Chang, C., Edirisinghe, I., White, K.D., Jablonski, J.E., Banaszewski, K., Kangath, A., Tadapaneni, R.K., Burton-Freeman, B., Jackson, L.S., 2012. Berry fruits modulated endothelial cell migration and angiogenesis via phosphoinositide-3 kinase/protein kinase B pathway in vitro in endothelial cells. J. Agric. Food Chem. 60, 5803–5812.
Velasco, I., Rueda, J., Acién, P., 2006. Aromatase expression in endometriotic tissues and cell cultures of patients with endometriosis. Mol. Hum. Reprod. 12, 377–381.
Wieser, F., Cohen, M., Gaeddert, A., Yu, J., Burks-Wicks, C., Berga, S.L., Taylor, R.N., 2007. Evolution of medical treatment for endometriosis: back to the roots? Hum. Reprod. Update 13, 487–499.
Zhao, D., Qin, C., Fan, X., Li, Y., Gu, B., 2014. Inhibitory effects of quercetin on angiogenesis in larval zebrafish and human umbilical vein endothelial cells. Eur. J. Pharmacol. 723, 360–367.